Super-resolution with Toraldo pupils: analysis with electromagnetic numerical simulations

Olmi, Luca, Bolli, Pietro, Cresci, Luca, Mugnai, Daniela, Natale, Enzo, et al.

Luca Olmi, Pietro Bolli, Luca Cresci, Daniela Mugnai, Enzo Natale, Renzo Nesti, Dario Panella, Lorenzo Stefani, "Super-resolution with Toraldo pupils: analysis with electromagnetic numerical simulations," Proc. SPIE 9906, Ground-based and Airborne Telescopes VI, 99065Y (27 July 2016); doi: 10.1117/12.2230970

SPIE.

Event: SPIE Astronomical Telescopes + Instrumentation, 2016, Edinburgh, United Kingdom

Super-resolution with Toraldo pupils: analysis with electromagnetic numerical simulations

Luca Olmi[a,b], Pietro Bolli[a], Luca Cresci[a], Daniela Mugnai[c], Enzo Natale[a], Renzo Nesti[a], Dario Panella[a], and Lorenzo Stefani[c]

[a]Istituto Nazionale di Astrofisica (INAF), Osservatorio Astrofisico di Arcetri, Largo E. Fermi 5, I-50125 Firenze, Italy

[b]University of Puerto Rico, Rio Piedras Campus, Physics Dept., Box 23343, UPR station, San Juan, Puerto Rico, USA

[c]Consiglio Nazionale delle Ricerche (CNR), Istituto di Fisica Applicata Nello Carrara, Via Madonna del Piano 10, I-50019 Firenze, Italy

ABSTRACT

The concept of super-resolution refers to various methods for improving the angular resolution of an optical imaging system beyond the classical diffraction limit. In optical microscopy, several techniques have been developed with the aim of narrowing the central lobe of the illumination Point Spread Function (PSF). In Astronomy a few methods have been proposed to achieve reflector telescopes and antennas with resolution significantly better than the diffraction limit but, to our best knowledge, no working system is in operation. A possible practical approach consists of using the so-called "Toraldo Pupils" (TPs) or variable transmittance filters. These pupils were introduced by G. Toraldo di Francia in 1952,[1] and consist of a series of discrete, concentric circular coronae providing specific optical transparency and dephasing in order to engineer the required PSF. The first successful laboratory test of TPs in the microwaves was achieved in 2003,[2] and in the present work we build upon these initial measurements to perform electromagnetic (EM) numerical simulations of TPs, using a commercial full-wave software tool. These simulations were used to study various EM effects that can mask and/or affect the performance of the pupils and to analyze the near-field as well as the far-field response. Our EM analysis confirms that at 20 GHz the width of the central lobe in the far-field generated by a TP significantly decreases compared to a clear circular aperture with the same diameter.

Keywords: Electromagnetic simulations, angular resolution, super-resolution techniques, Toraldo pupils

1. INTRODUCTION

The concept of super-resolution refers to various methods for improving the angular resolution of an optical imaging system beyond the classical diffraction limit. In optical microscopy, several techniques have been successfully developed with the aim of narrowing the central lobe of the illumination Point Spread Function. These techniques either involve changing the fluorescence status of the specimen, or the specimen is imaged within a region having a radius much shorter than the illumination wavelength, thus exploiting the unique properties of the evanescent waves. Interference microscopy is also used*.

In Astronomy no technique equivalent to either fluorescence (far-field) or near-field microscopy can be used. In the past, the most common method proposed for designing super-resolving pupils for optical telescopes employed either *variable transmittance pupils* or phase masks.[5,6] In more recent years, more "exotic" techniques have also been proposed, employing for example quantum cloning[3] or negative refractive index materials.[4] However, none of these methods has been further analyzed and tested beyond the stage of basic principles.

Further author information: (Send correspondence to L.O.)
L.O.: E-mail: olmi.luca@gmail.com
P.B.: E-mail: pbolli@arcetri.astro.it
D.M.: E-mail: d.mugnai@ifac.cnr.it

*see, e.g., http://zeiss-campus.magnet.fsu.edu/articles/superresolution/introduction.html

Ground-based and Airborne Telescopes VI, edited by Helen J. Hall, Roberto Gilmozzi, Heather K. Marshall,
Proc. of SPIE Vol. 9906, 99065Y · © 2016 SPIE · CCC code: 0277-786X/16/$18 · doi: 10.1117/12.2230970

The first time that variable transmittance pupils were discussed was at a lecture delivered by Toraldo di Francia at a colloquium on optics and microwaves in 1952.[1] Toraldo di Francia suggested that the classical limit of optical resolution could be improved interposing a filter consisting of either infinitely narrow concentric rings or finite-width concentric annuli of different amplitude and phase transmittance in the exit pupil of an optical system. These pupils are now also known as Toraldo variable transmittance pupils (TPs, hereafter). Many other super-resolving filters have since been proposed, but these methods offer little theoretical advantage over the original method proposed by Toraldo di Francia, as shown in Ref. 7.

The first experimental studies, in the microwave range, of a TP have been carried out in 2003[2] and 2004.[8] These successful results raised the interest in the potential application of TPs to microwave antennas and radio telescopes. For this reason we started a project devoted to a more careful analysis of TPs and how they could be implemented on a radio telescope. The purpose of this paper is thus to discuss the results of extensive electromagnetic (EM) numerical simulations of TPs, using a commercial full-wave software tool. We use these simulations to study various EM effects that can mask and/or modify the performance of the pupils and to analyze the near-field as well as the far-field response. We also used these EM simulations to prepare more comprehensive laboratory testing, with the final goal to design a prototype TP to be mounted on a radio antenna.

2. TORALDO PUPILS

2.1 Analytical description

As originally shown by Toraldo di Francia[1] and later discussed by other authors,[2,7,9] let us consider a circular pupil of diameter D and divide it into n discrete, concentric circular coronae by means of $n+1$ circumferences with diameters $\alpha_0 D$, $\alpha_1 D$, ..., $\alpha_n D$, where α_0, ..., α_n is a succession of numbers in increasing order, with $\alpha_0 = 0$ and $\alpha_n = 1$. In its original and simplest configuration, each corona is either perfectly transparent or provides a phase inversion (i.e., a $\Delta\phi = 180^\circ$ phase change). By setting $x = \pi \frac{D}{\lambda} \sin\theta$, where θ is the angle of diffraction measured with respect to the optical axis and λ is the wavelength, it can be shown that the total (far-field) amplitude, $A(x)$, diffracted by the composite TP is given by:

$$A(x) = \sum_{i=0}^{n-1} \frac{k_{i+1}}{x} [\alpha_{i+1} J_1(\alpha_{i+1} x) - \alpha_i J_1(\alpha_i x)] \tag{1}$$

where $k_{i+1} = \frac{\pi D^2}{2\lambda^2} A_{i+1}$ is a constant that is proportional to the amplitude A_{i+1} illuminating each corona, and J_1 is the Bessel function of the first order. Once the partition of the pupil into a number of circular coronae is established, we can impose n independent conditions on Eq. (1) (for instance, the x values of its zeros), thus obtaining a system of n equations from which we can determine the coefficients $k_1, ..., k_n$. Note that the k coefficients can also have negative values, in which case they represent a *phase-inversion* of the wave propagating through the pupil. We have not yet simulated the most general type of variable transmittance pupils with both amplitude *and* phase variation over the aperture. In order to obtain the phase-inversion, $\Delta\phi = (2\pi/\lambda)\,\Delta l = \pi$, the optical path *excess* (with respect to the wave propagating through air), $\Delta l = n\,\Delta s$ where Δs is the physical thickness and n is the refraction index, must be equal to $\Delta l = 1.5\lambda$ (and not just $\Delta l = 0.5\lambda$).

2.2 Example of TP with 3 coronae at 20 GHz

Let us now consider the simple case of a three-coronae TP with the radii in arithmetic progression,[2] $\alpha_0 = 0$, $\alpha_1 = 1/3$, $\alpha_2 = 2/3$ and $\alpha_3 = 1$. Given our interest in the potential application of TPs to radio antennas, most of our analysis has been carried out at a nominal frequency of 20 GHz. As discussed in the previous section, we must now set three conditions on $A(x)$ in order to derive the three k_i coefficients. Given that an open pupil with the same diameter has its first zero at $x = 3.83$ (corresponding to $\sin\theta = 1.22\lambda/D$) we set the three conditions $A(x=0) = 1$, $A(x=2) = 0$ (thus narrowing the main lobe) and $A(x=3.8) = 0$, similar to those used by Toraldo di Francia[1] in one of his examples. We then find that $k_1 = 68.3$, $k_2 = -43.4$ and $k_3 = 16.0$, and Fig. 1 shows the diffracted intensity and required illumination. Specifically, the left panel shows how the full width at half maximum (FWHM) of the central lobe of the TP has been reduced (by a factor of $\simeq 2.5$) compared to the open pupil, accompanied by a significant increase in the intensity of the sidelobes. The middle panel of Fig. 1 shows the pupil (amplitude) illumination required by the k-coefficients, which ideally is supposed to be uniform

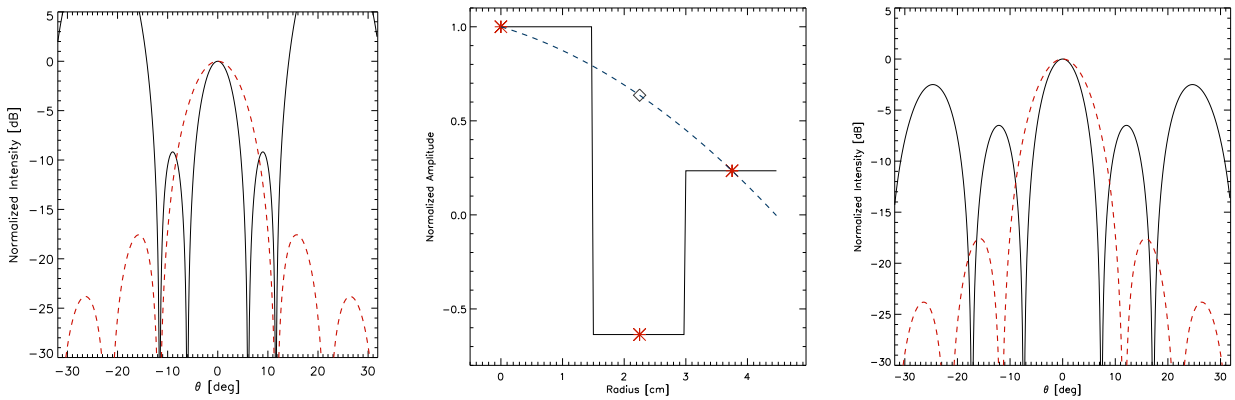

Figure 1. *Left panel.* Diffraction pattern at $\nu = 20\,\mathrm{GHz}$ by a three-coronae TP, as given by the square of Eq. (1) for $n = 3$ (black solid line), and that of a normal pupil of equal diameter (red dashed line). Both curves are normalized with respect to the on-axis value. The gain in angular resolution, as measured by the ratio of the widths of the central lobe, is a 2.5 factor. *Middle panel.* Pupil illumination as required by the k-coefficients in Eq. (1). The red "*" symbols represent the relative magnitudes of k_1, k_2 and k_3, with the diamond symbol corresponding to $|k_2|$. The blue dashed line represents the best-fit Gaussian illumination, assuming all positive k values. *Right panel.* Normalized diffraction pattern at $\nu = 20\,\mathrm{GHz}$ assuming a plane wave (uniform phase) illumination. The gain in angular resolution is a 2.0 factor.

over each separate corona. As far as the phase is concerned, the illumination of a TP requires a uniform phase (i.e., a plane wave) except on those coronae with negative k-coefficients, which require a phase inversion.

The simple 3-coronae example of Fig. 1 also shows that the geometry of the TP can be chosen so that the required intensity illumination at the center of each corona can be adequately fit by a Gaussian beam. Gaussian illumination can be easily obtained using a feedhorn (see Sect. 3.3), but a Gaussian beam cannot provide simultaneously also a uniform phase over the pupil. Alternatively, if the pupil is located in the far-field of the Gaussian beam source, the spherical wavefront can be approximated as a plane wave over the extent of the pupil, thus satisfying the uniform phase condition but without the required amplitude apodization. The right panel of Fig. 1 shows the different far-field obtained when the 3-coronae TP is illuminated with a *plane wave* (still satisfying the phase inversion condition). Compared to the distribution shown in the left panel, two main differences are immediately visible: first, the central lobe is wider, thus loosing some of the super-resolution effect. Then, the relative strength of the various sidelobes is changed, and the central lobe is now more intense. We have also verified that maintaining the uniform phase condition over the pupil is more important, to achieve the super-resolution effect, than achieving the correct beam-apodization, as for example shown in the middle panel of Fig. 1.

In this work we will focus our discussion on the simplest example of TP, i.e. the pupil with 3 coronae, because the EM simulations are less demanding and also because it is easier to model analytically. As the number of circular coronae is increased, the user has more parameters to adjust both the level of super-resolution achieved *and* the level of the sidelobes. A full discussion of the 4-coronae TP will be given elsewhere (Olmi *et al.*, in prep.), however in Sect. 3.5 we give a brief example of performance of this pupil.

3. ELECTROMAGNETIC SIMULATIONS

3.1 Rationale

The analytical description of the TP discussed in the previous section refers to an ideal optical system where several implicit assumptions have been made, specifically:

- the opaque plane containing the pupil extends to infinity and is infinitesimally thin;
- likewise, the phase inversion, where required, is obtained using infinitesimally thin optical transmittance filters;

- an ideal source is assumed that achieves both the required amplitude apodization and uniform phase illumination over the pupil;
- the total diffracted amplitude given by Eq. (1) is only valid in the far-field of the pupil.

Any measurement performed in the laboratory cannot fully satisfy all of the previous optically ideal conditions, and thus a way to validate and test the performance of a TP under less than ideal lab conditions is required. The method used must also be able to address how the theoretical performance of a TP can be masked or altered by various optical (mostly diffractive) effects.

Therefore, we carried out an extensive series of EM numerical simulations using the commercial software FEKO[†] (see Sect. 3.2), a comprehensive EM simulation software tool for the electromagnetic field analysis of 3D structures. During the initial phases of this project we also used GRASP[‡], another well-known commercial software that specializes in the precise modelling of reflector antennas. The simulations described here had the main purpose of generating a FEKO model as close as possible to the ideal optical system described by the previous assumptions, thus trying to test the performance predicted by Eq. (1). In a following paper (Olmi *et al.*, in preparation) we will discuss the simulation of laboratory measurements which had the main goal of testing how the ideal performance of a TP would be modified under more realistic conditions. These simulations also had the purpose to compare the near- and far-field results, given that all laboratory measurements would take place in the near-field of the TP.

3.2 Basic parameters of the EM simulations

The EM numerical results described in this work were obtained with the commercial software FEKO, which offers a wide number of tools and solvers for addressing specific EM problems. During the initial phases of this project, we focused on how to model and analyze the TP system within FEKO. Specifically, we concentrated on modeling the infinite ground plane and on the implementation of the required aperture illumination. As we also describe later in Sect. 3.3, we found that the most efficient way, in terms of computational resources and accuracy, to model a circular aperture in an infinite plane consisted of using a "*planar multi-layer substrate*" (PMS) solved by planar Green's functions. This approach eliminates the diffraction effects from the external edges of the finite ground plane and thus it allowed us to use a simple plane wave as the aperture illumination. However, we verified that using tapered excitation, as for example provided by a rectangular feedhorn (see Sect. 3.6), the resulting amplitude distribution provides quite similar results to those obtained with a plane wave. In our simulations, the dielectric circular coronae of the TP were solved with the default method recommended by FEKO for dielectric media. This method, using the surface equivalent principle, introduces equivalent electric and magnetic currents on the surface of the dielectric component.

We verified that a "coarse" mesh size was able to correctly model the geometry of our system. The 3-coronae TP model at 20 GHz was simulated by FEKO in about 2 hours with 7 parallel processors[§]. During our initial tests, we also used a finite circular disk to approximate the infinite screen. In order to minimize the diffraction effects from the external edge of the disk, we used a tapered excitation combined with a disk whose diameter was such that the edge illumination was at least $-10\,\mathrm{dB}$ lower with respect to the on-axis intensity. In this case, the Multilevel Fast Multipole Method (MLFMM) was found to be the most efficient numerical method for such electrically large structures. The main idea behind the MLFMM is to group individual basis functions and to use them to compute the interaction between different parts of the model.

3.3 Illuminating source and edge diffraction

During the EM simulations our illuminating sources were mainly plane waves and Gaussian beams. The near-field of a circular or rectangular feedhorn can be approximated as a Gaussian beam, and we simulated the feedhorn fields directly in FEKO, using the "aperture excitation" technique, which then allowed us to apply the same source field to different models. As previuosly mentioned, plane waves meet the uniform phase conditions, but

[†]http://www.altairhyperworks.com/product/FEKO
[‡]http://www.ticra.com/products/software/grasp
[§]XEON CPU E3-1275 V2@3.5 GHz with 32 GB RAM

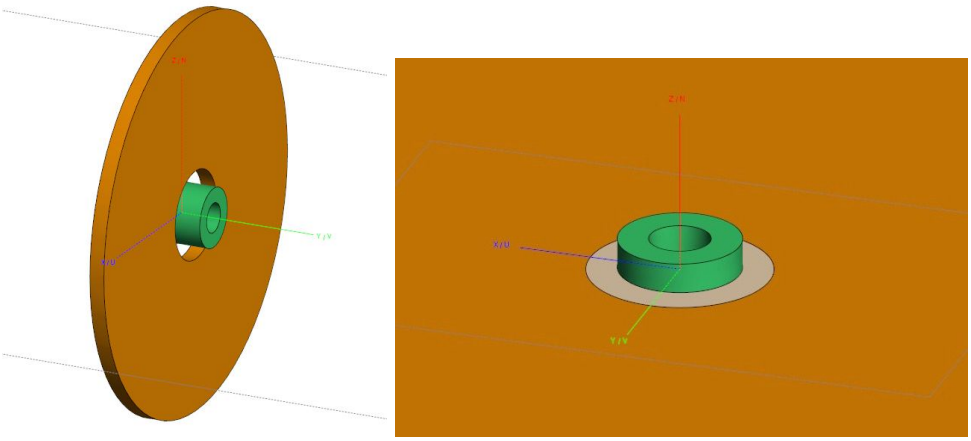

Figure 2. *Left panel.* Initial FEKO model used to simulate a 3-coronae TP at 20 GHz. The green cylinder represents the dielectric layer (with refractive index $n = 1.5$) employed to implement the phase inversion. The open pupil has a diameter of 9 cm, and the radii of the four circumferences delimiting the three coronae are 0, 1.5, 3.0 and 4.5 cm. *Right panel.* FEKO model for a 3-coronae TP using the planar multilayer substrate option simulating an infinite opaque screen.

not the amplitude apodization. Gaussian beams in general do not meet either condition, but if the illuminated pupil is positioned in the far-field of the source, the phase ϕ over the limited extent of the pupil can be made uniform to within $\Delta\phi \ll 1$ rad. At the same time the beam naturally provides an amplitude taper beyond the pupil extent.

Since in Section 2.2 we mentioned that the uniform phase condition is more relevant to achieve the super-resolution effect of a TP than the beam apodization, we decided to work initially with plane waves as our source of illumination. However, plane wave have a serious drawback when working in the near-field with finite-edge elements. Figure 2 shows the initial model used to simulate a 3-coronae TP using a conductive metal disk with a finite diameter as the opaque screen. If plane waves are used as illuminating source, diffraction by the disk edge is very significant and generates various diffraction peaks in the near-field along the optical axis, which can mask the super-resolution effect. On the other hand, when using a Gaussian beam source with the same model, in order to taper down the amplitude at the edges of the disk while still maintaining an acceptable uniform phase over the pupil, the disk diameter may have to be increased to many tens of wavelengths. However, a trade-off must be obtained between the desired edge-taper and the resulting computational time, which may quickly increase when using larger disks.

Figure 3 shows the different near-field amplitude distributions obtained when using a plane wave and Gaussian incident fields[¶]. In the panel on the left the multiple diffraction rings generated by the diffraction of the plane wave at the edge of the disk are clearly visible. In the right panel of Fig. 3 we used instead a rectangular feedhorn (described in Sect. 3.6) as the illuminating source. Clearly, the tapered amplitude field incident on the circular disk does not generate visible diffraction effects. We have also verified that the edge diffraction effects are not much dependent on the *shape* of the screen. The disk shown in Figures 2 and 3 has a radius of 20 cm, i.e. $\simeq 13\,\lambda$. We have verified that given the taper level, even doubling the disk radius does not change the output field significantly. Therefore, a feedhorn that generates a tapered Gaussian beam has been used to simulate the performance of a TP under laboratory conditions (see Sect. 3.6).

Instead, when using plane waves, the diffraction effects may mask any super-resolution amplitude distribution in the near-field. To overcome this problem and still being able to use plane waves as illuminating source we have instead adopted the PMS option in FEKO described in Sect. 3.2. The use of this method allows the numerical simulation of the far-field generated by a TP under conditions closer to those required by the ideal optical assumptions leading to Eq. (1).

[¶]This and the subsequent figures always show the amplitude of the *electric* field.

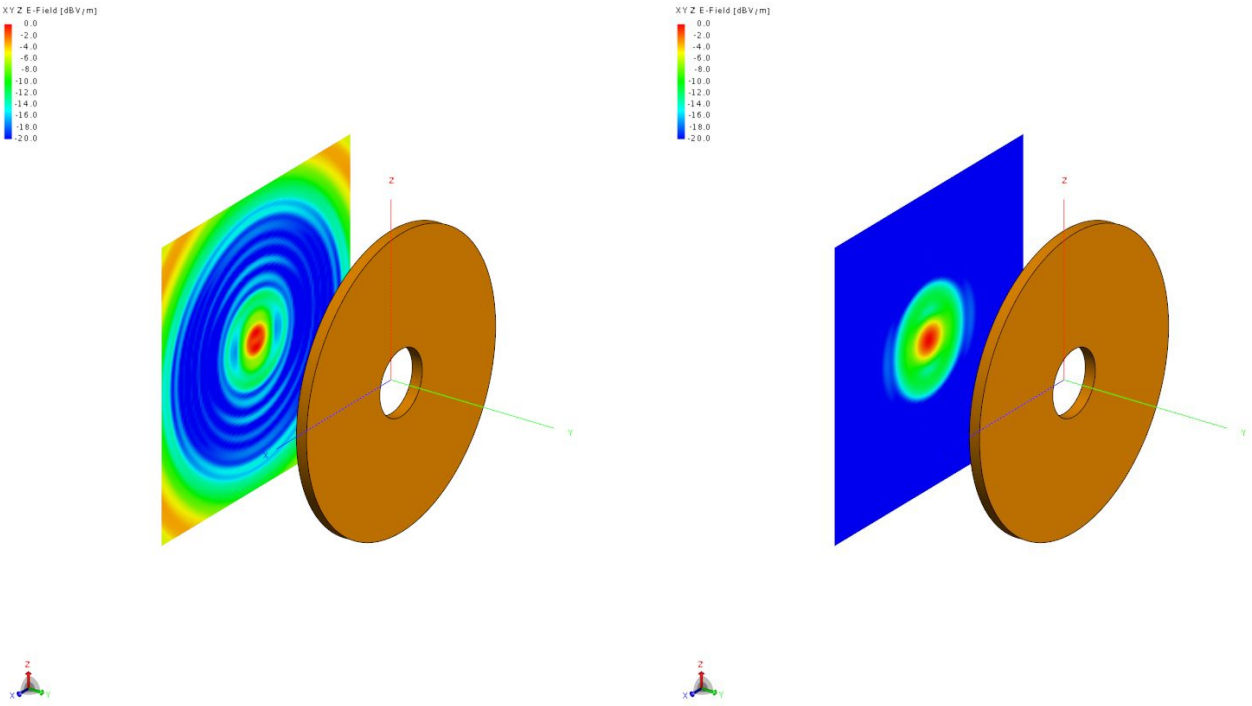

Figure 3. *Left panel.* Modeled distribution of the near-field at 20 GHz for the 3-coronae TP using an incident plane wave (incident from the right). Multiple diffraction rings are visible. The open pupil and the circular screen have a diameter of 9 cm and 40 cm, respectively, while the distance between the screen and the plane where the near-field has been computed is 20 cm. The screen thickness is one wavelength ($\simeq 1.5$ cm). *Right panel.* Same as above for an incident field generated by a rectangular feedhorn with edge taper (see text). The edge diffraction effects have disappeared. The logarithmic color scale (from -20 dBV/m, blue, to 0 dBV/m, red) is the same for both figures.

3.4 EM simulations with plane waves and PMS option

Our initial EM numerical simulations were then performed using a plane wave illumination and the PMS option to implement an infinite ground screen. We estimated both the near- and far-fields, with the near-field being simulated at different distances from the TP in order to evaluate the fast-varying characteristics of the field. The near- and far-fields are shown in Figures 4 and 5, respectively, where they are also compared with the field distribution obtained with an open pupil having the same diameter as the TP, and also with the far-field of a 4-coronae TP (see Sect. 3.5). The super-resolution effect can be clearly seen in the central lobe of the far-field radiation diagram, where the FWHM of the main lobe has been reduced by a $\simeq 1.5$ and $\simeq 1.3$ factor for the 3- and 4-coronae TPs, respectively. The resolution gain factor for the 3-coronae TP is lower compared to the value listed in Fig. 1 (right panel) and, as discussed in Sect. 3.1, is a consequence of the differences between the ideal optical system and the more realistic model simulated with FEKO.

Since the illuminating source is a plane wave, with no beam amplitude apodization, this figure can also be compared with the analytical result shown in the right panel of Fig. 1. One can note the qualitative similarity between the analytical and numerical results, although the relative levels of the sidelobes are not exactly the same. The main differences between the analytical and FEKO models reside in the finite thickness of the dielectric layer used to implement the phase inversion, and in its discretization (as given by the mesh discussed in Sect. 3.2) in the FEKO model.

3.5 Toraldo pupil with 4 coronae

As we mentioned in Sect. 2.2 a 4-coronae TP, though more complicated to analyze, gives more flexibility in terms of design-space parameters. The example of a 4-coronae TP in Fig. 5 shows how the increased number

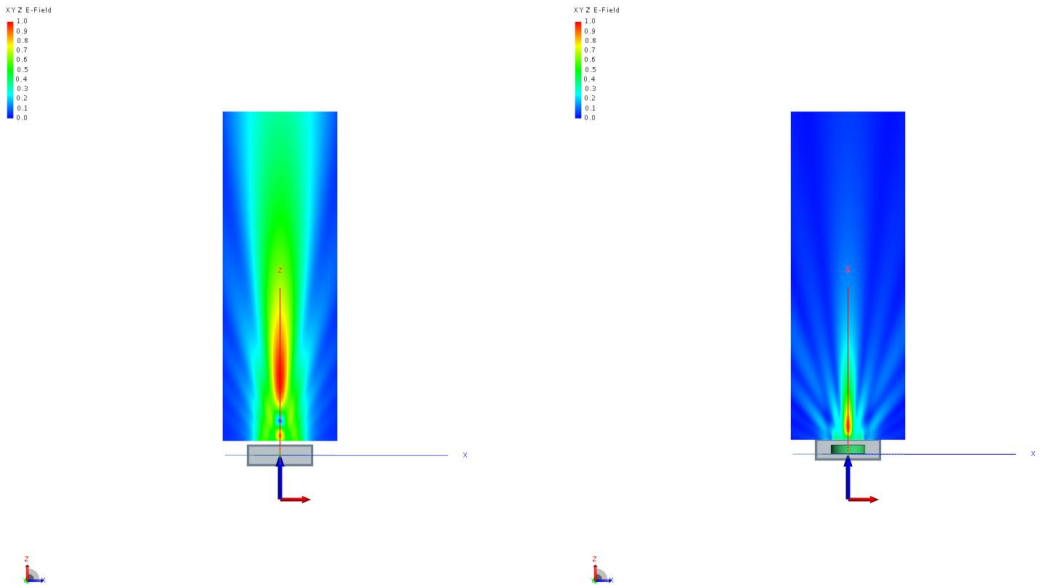

Figure 4. Modeled distribution of the near-field at 20 GHz for the open pupil (left) and for the 3-coronae TP (right). The corresponding far-fields are shown in Fig. 5 together with the far-field of a 4-coronae TP, for comparison. The normalized (red corresponds to 1) and linear color scale is the same for both figures. The equivalent infinite opaque screen generated by the PMS option corresponds to the xy plane, i.e. perpendicular to the plane of the figure.

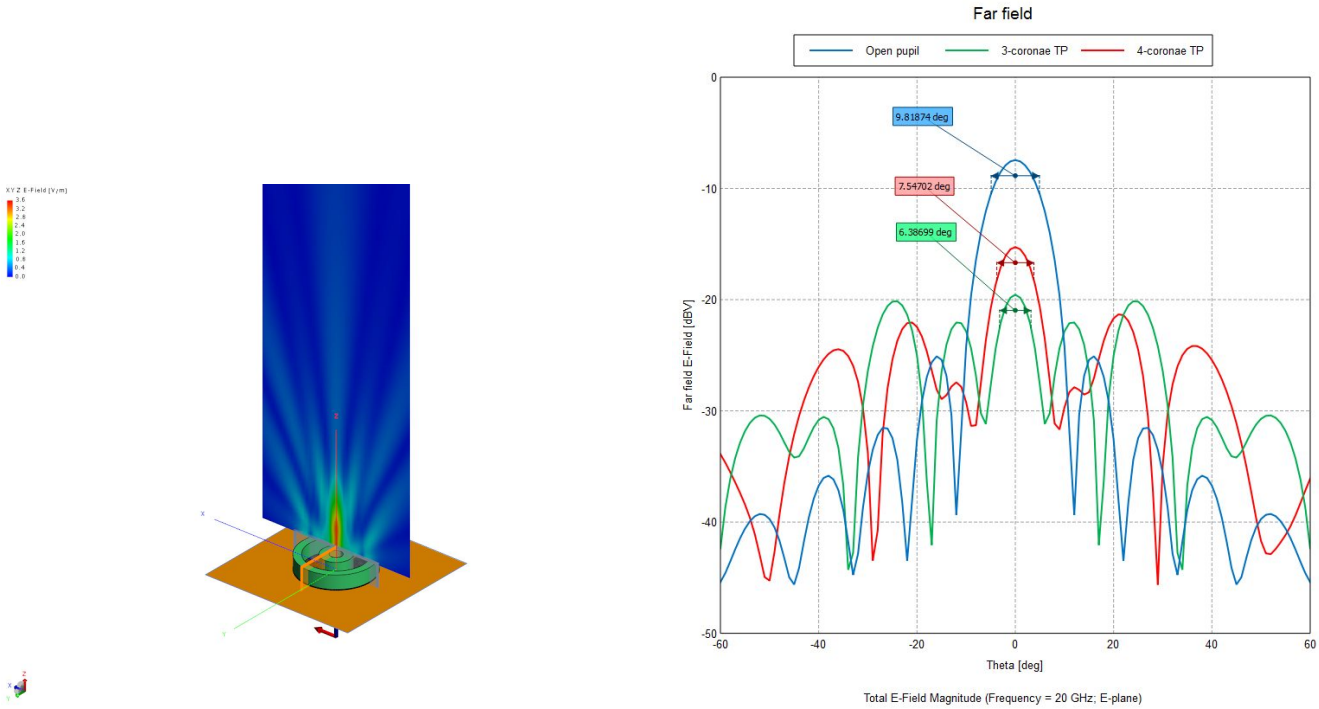

Figure 5. *Left panel.* Modeled distribution of the near-field at 20 GHz for the 4-coronae TP. The two green rings show the dielectric material. *Right panel.* Plot of the amplitude in the far-field (red line), which also shows the comparison with the amplitude distributions of the open pupil (blue line) and 3-coronae TP (green line). A plane wave and the PMS option (which generates the opaque screen shown as a brown background in the left panel) were used.

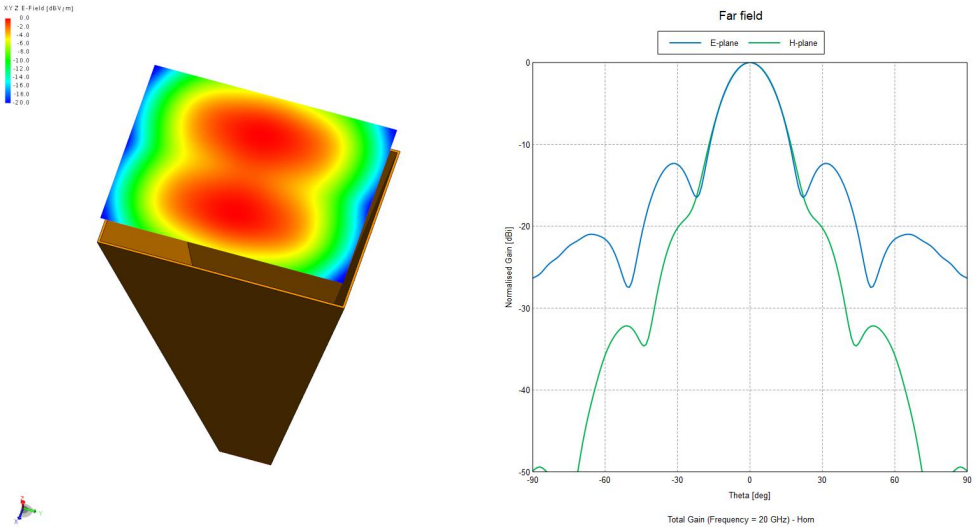

Figure 6. *Left panel.* Distribution of the field amplitude at the mouth of the rectangular feedhorn described in the text. The color scale is the same as in Fig. 3. *Right panel.* Far-field of the feedhorn, along the E- (blue line) and H-planes (green line).

of coronae can be used in the trade-off of various design parameters. In this specific example the radii of the coronae were selected such that the required illumination, according to Eq. (1), is almost Gaussian. In this case, the phase inversion must take place on the 2nd and 4th corona, as shown by the dielectric cylinders in the left panel of Fig. 5 and, as in the case of the 3-coronae TP, we adopted a plane wave illumination. The far-fields of the three configurations show that increasing the number of coronae can, for example, reduce the strength of the sidelobes, though at the cost of increasing the FWHM of the central lobe. It is thus conceivable that by further increasing the number of coronae even a better trade-off could be achieved, though clearly at the additional cost of increasing absorption by the dielectric filters.

3.6 EM simulations with Gaussian beams

When switching from plane waves to more realistic sources, such as a rectangular feedhorn, we found out that the PMS option of FEKO cannot be used. We therefore separately simulated the feedhorn in FEKO and then saved the fields on the horn aperture as an "aperture excitation" file. These fields were then imported back in FEKO and used as source to illuminate the PMS ground screen.

Using the aperture excitation method we simulated a rectangular feedhorn having a mouth 4×5.5 cm in size, while the waveguide had dimensions 1.07×0.43 cm with a total length of 11 cm. Thus, the horn had a taper of -3 dB at an angle of $\simeq 9$ deg with respect to the optical axis, and a gain of $\simeq 20$ dB (see Fig. 6). Using this horn as an illuminating source, we found that the phase variation over the aperture of the 3-coronae TP discussed above is $\simeq 12$ deg, or 0.2 rad at a distance of about 2 m. This is the value to be expected for a spherical wave of radius 2 m, and this phase variation is sufficiently small that the far-field generated by the pupil is basically the same as obtained with the plane waves. The far-fields obtained with plane wave and feedhorn illuminating sources are shown in Fig. 7, where the resulting amplitude distributions are almost identical.

3.7 EM simulations including antenna

Since our final goal is to design a prototype TP to be mounted on an existing radio telescope, our next step consisted in simulating a full optical system, including an antenna as the first element. We chose as reference antenna the 32-m Medicina radio telescope[‖], and from the optical parameters of this antenna we generated its equivalent paraboloid, which we also simulated in FEKO. However, given the excessive simulation time required

[‖] http://www.med.ira.inaf.it/index_EN.htm

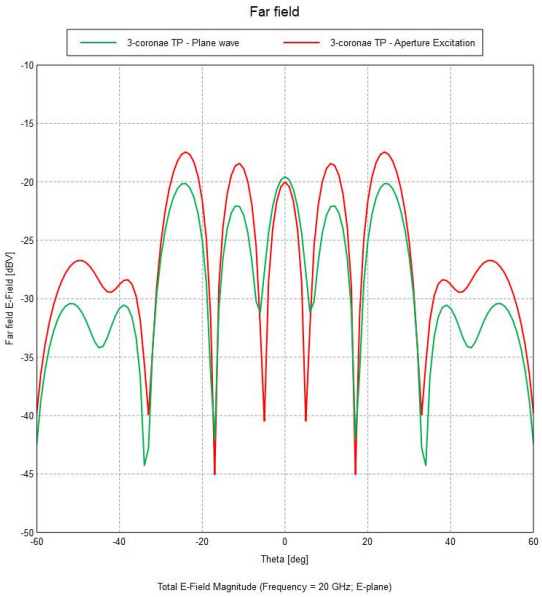

Figure 7. FEKO simulation showing the amplitude of the far-field at 20 GHz for the 3-coronae TP model, using the two configurations shown in Fig. 2, i.e., a rectangular feedhorn source whose field is incident on a circular finite screen (red curve, with higher sidelobes), and a plane wave with the PMS option (green curve).

for a 32-m aperture antenna, we decided to limit the aperture to just 3.2-m, while maintaining the same system focal ratio (so that $f = 9.72$ m), thus leading to the same physical size of the point spread function at the focus of the equivalent paraboloid.

The fields generated at the focus of the equivalent paraboloid were then converted into an "aperture excitation" file, as described earlier, and then imported back into FEKO (see Fig. 8). The source fields are allowed to re-expand and the expanding spherical wavefront is converted into a plane wave by a lens whose focus coincides with the input illumination source. This plane wave is then used as illuminating source of the 3-coronae TP, which is then located at an image of the entrance pupil (the telescope aperture). The resulting far-field after the TP is shown in Fig. 9. This figure clearly shows that the super-resolution effect is achieved in the far-field of the

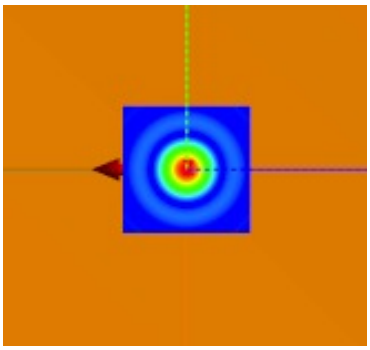

Figure 8. 2-D amplitude distribution of the "aperture excitation" fields obtained at the Cassegrain focus of the equivalent paraboloid (see text). The square area displayed measures 20 cm on a side, and the color scale is the same as in Fig. 4.

TP, with results similar to those obtained when a direct source of plane waves is used. However, we note that the gain in angular resolution, as measured by the ratio of the widths of the central lobe for the open pupil and the TP, is $\simeq 2$, *higher* than that shown in Fig. 5. The intensity ratio of the side lobes to the main lobe is also different. Though we have not further investigated this discrepancy we think it is likely caused by a different

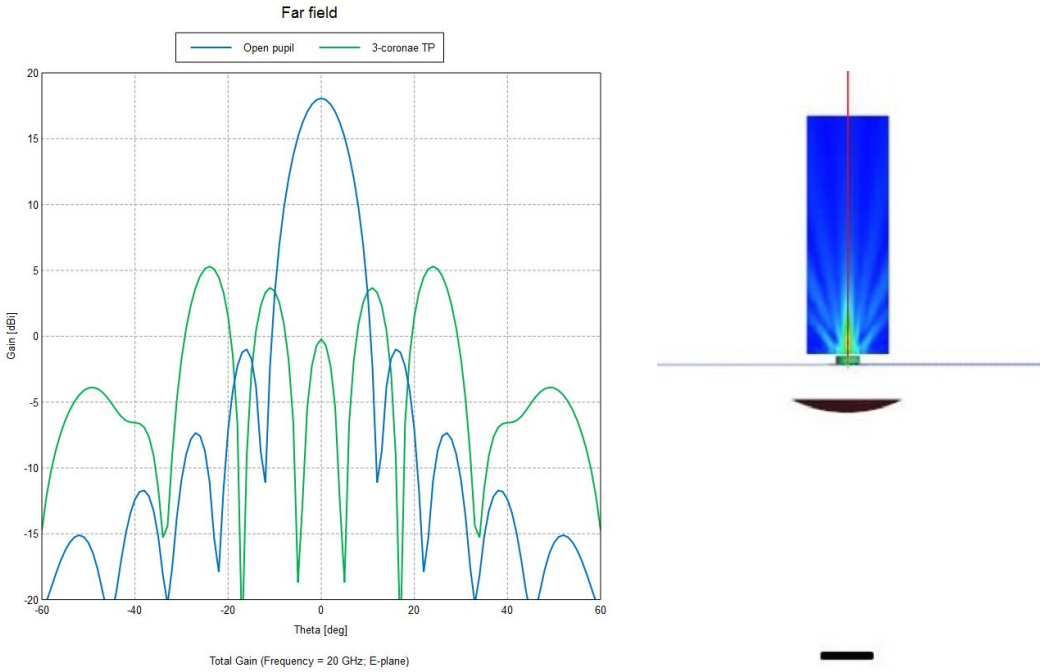

Figure 9. *Left panel.* FEKO simulation showing the amplitude of the far-field at 20 GHz for the 3-coronae TP model (green line), using as a source the equivalent "aperture excitation" fields obtained at the Cassegrain focus of an antenna whose aperture diameter was 3.2 m and the same f/D as the Medicina antenna (hence $f = 9.72$ m). Shown for comparison is also the far-field of the open pupil (blue line). *Right panel.* The optical system used in this simulation. The black bar at the bottom represents the Cassegrain focus (see Fig. 8), which coincides with the focus of the plano-convex lens. This lens converts the expanding spherical wave into a plane wave that intercepts a TP and generates the near-field shown. The lens has a radius of curvature of 28 cm, a diameter of 25 cm and a thickness along the optical axis of 3 cm. The separation between the lens and the PMS screen has been reduced in the figure for the sake of clarity. The real distance used for this simulation was 150 cm. The color scale and the infinite opaque screen are the same as in Fig. 4. The gain in angular resolution, as measured by the ratio of the widths of the central lobe, is a $\simeq 2$ factor.

amplitude and phase illumination of the pupil. Finally, in order for this optical system to be able to work with a radio receiver, the collimator needs to be completed with a second lens positioned after the TP, which can modify the transformed plane wave into a converging spherical wave to illuminate the feedhorn of the receiver.

4. CONCLUDING REMARKS AND FUTURE WORK

We have carried out an extensive set of numerical EM simulations that analyze the optical performance of the simplest types of TP in both the near- and far-fields. The simulations confirm the analytical predictions of Ref. 1. These simulations also allowed us to analyze the performance of TPs when some of the ideal optical assumptions, required by the analytical analysis, must be relaxed. Finally, we have used these simulations to model a complete optical system including both a Cassegrain radio telescope and a collimator. In fact, as we mentioned in the Introduction, our main interest for TPs lies in their potential application to microwave antennas and radio telescopes. Therefore, the EM simulations discussed here were the first step of a more comprehensive project which includes an extensive laboratory testing of the performance of both 3- and 4-coronae TPs. These experimental tests have been successfully carried out and a complete report will be presented elsewhere (Olmi *et al.*, in preparation). We are also planning a first series of field tests, where we will design and mount a proof-of-concept prototype on a radio telescope employing a K-band receiver.

We are also currently working on some interesting theoretical aspects related to the super-resolution achieved with a TP, as well as to the possible applications of metamaterials (for a review see, e.g., Ref. 10) to the design and fabrication of more efficient TPs. In fact, the determination of an optimum TP for a specific

optical application, in accordance with a set of pre-specified requirements for amplitude and phase distribution around the focus, constitutes a problem of nonlinear optimization (see, e.g., Ref. 11). However, besides to the optimization procedure an equally efficient fabrication technique would be required to practically implement the optimized designs.

REFERENCES

[1] Toraldo di Francia, G. *Atti Fond. Giorgio Ronchi* **7**, 366 (1952).

[2] Mugnai, D., Ranfagni, A., and Ruggeri, R., "Pupils with super-resolution," *Physics Letters A* **311**, 77–81 (May 2003).

[3] Kellerer, A., "Beating the diffraction limit in astronomy via quantum cloning," *Astronomy and Astrophysics* **561**, A118 (Jan. 2014).

[4] May, J. and Jennetti, T. in [*UV/Optical/IR Space Telescopes: Innovative Technologies and Concepts*], MacEwen, H. . A., ed., *Proc. SPIE* **5166**, 220 (2004).

[5] Cagigal, M. P., Canales, V. F., and Oti, J. E., "Design of Continuous Superresolving Masks for Ground-based Telescopes," *Publications of the Astronomical Society of the Pacific* **116**, 965–970 (Oct. 2004).

[6] Canales, V. F., de Juana, D. M., and Cagigal, M. P., "Superresolution in compensated telescopes," *Optics Letters* **29**, 935–937 (May 2004).

[7] Cox, I. J., Sheppard, C. J. R., and Wilson, T., "Reappraisal of arrays of concentric annuli as superresolving filters," *Journal of the Optical Society of America (1917-1983)* **72** (Sept. 1982).

[8] Ranfagni, A., Mugnai, D., and Ruggeri, R., "Beyond the diffraction limit: Super-resolving pupils," *Journal of Applied Physics* **95**, 2217–2222 (Mar. 2004).

[9] Born, M. and Wolf, E., [*Principles of Optics*], seventh ed. (Oct. 1999).

[10] Lu, D. and Liu, Z., "Hyperlenses and metalenses for far-field super-resolution imaging," *Nature Communications* **3**, 1205 (Nov. 2012).

[11] Hazra, L. N. and Reza, N., "Optimal design of Toraldo super-resolving filters," in [*Novel Optical Systems Design and Optimization XIII*], *Proc. SPIE* **7787**, 77870D (Aug. 2010).